Report No.- Restricted

Report

X ray imaging for fish counting

Author(s) : Grégory Bouquet, Odd Løvhaugen, Marion O´Farell, Trine Kirkhus, Karl Henrik Haugholt, Alain Ferber

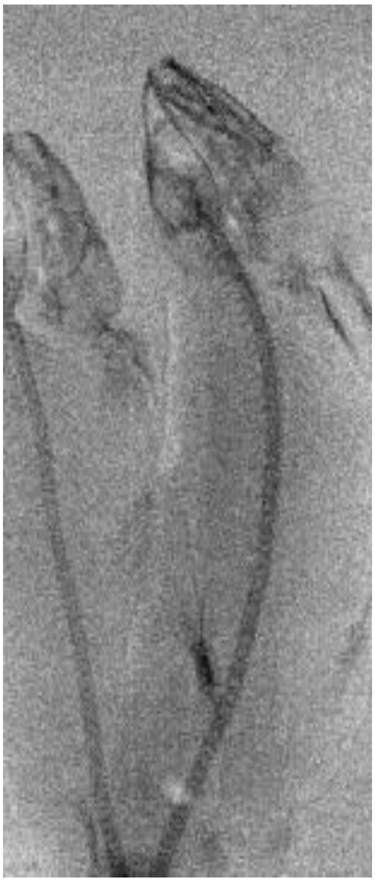

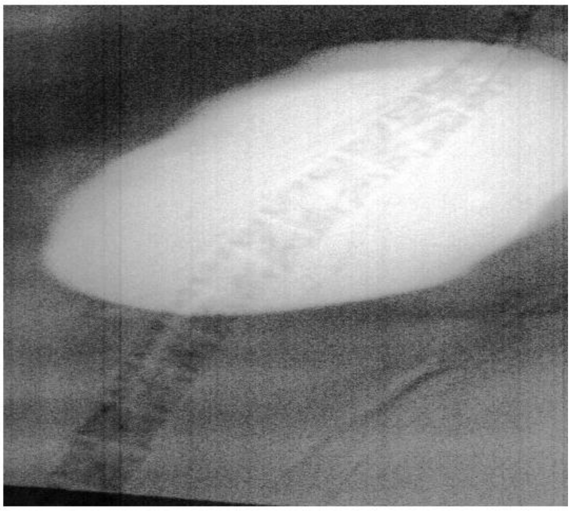

SINTEF ICT
Optical Measurements and Data Analysis
Date

SINTEF IKT
SINTEF ICT
Address:
Postboks 124 Blindern
NO-0314 Oslo
NORWAY
Telephone:+47 73593000
Telefax:+47 22067350
postmottak.IKT@sintef.no
www.sintef.no
Enterprise /VAT No:
NO 948 007 029 MVA

KEYWORDS:
Aquaculture,
Optical Measurement Systems and Data Analysis,
Fish counting,
X-ray imaging

Report

X ray imaging for fish counting

VERSION	DATE
Version No.2	Date

AUTHOR(S)
Grégory Bouquet
Odd Løvhaugen, Marion O´Farell, Trine Kirkhus, Karl Henrik Haugholt, Alain Ferber

CLIENT(S)	CLIENT'S REF.
SINTEF Fisheries and Aquaculture	Client's reference
PROJECT NO.	**NUMBER OF PAGES/APPENDICES:**
90J36601	33 + Appendices

ABSTRACT

Abstract

This rapport documents the possibility of using X-ray imaging as a method for detecting and counting fish in a fish counting system. The purpose of the research was to investigate and document the potential of x-ray since other techniques were hampered by the water level and turbidity in the pipes and x-ray has greater penetrating power to deal with this. X-ray has also the potential to distinguish between several overlapping fishes in the pipe and as a consequence should offer a better precision on the biomass estimation.

The laboratory results show that it is possible to detect small to large fishes (800-5 000 grams) in small to large amount of water (15 cm to 35 cm tube diameter) at a speed of at least 1 meters per second with a high spatial resolution (1 mm) and a rather compact and low cost set up. Higher speed could be achieved at the expense of a lower spatial resolution. Given the large size of the fishes that have to be detected, multiplying the spatial resolution by a factor of 2 to 4 will not affect too much the image quality. It has also been verified that imaging the fishes bones, allowed detecting overlapping fishes (2 to 4) even when a large amount of water is used. This is a consequence of the similar x-ray attenuation of fish muscle and water. Typical application could be pumping of smolt to the production pens or counting of large fishes before slaughtering.

PREPARED BY	SIGNATURE
Grégory Bouquet	Grégory Bouquet
CHECKED BY	**SIGNATURE**
Odd Løvhaugen	Odd Løvhaugen
APPROVED BY	**SIGNATURE**
Mats Carlin	

REPORT NO.	ISBN	CLASSIFICATION	CLASSIFICATION THIS PAGE
SINTEF F23838	ISBN	Restricted	Restricted

Document history

VERSION	DATE	VERSION DESCRIPTION
Version No.1	2012-06-11	First sketch
Version No.2	2013-01-07	First revision

Table of contents

Summary of the results 4

1 Simulation of a x-ray based fish counting system 6

1.1 Description of the simulation set up 6

1.1.1 Interaction of x-ray with matter and material parameters 6

1.1.2 Simulation set up 7

1.1.3 Fotodiode response 8

1.2 Identification of optimal source voltage 9

1.3 Effect of air bubbles 12

1.4 Effect of the scintillator thickness on contrast and SNR 12

1.5 Simulation on small fishes 14

1.6 Spatial resolution 15

1.7 Summary of the simulation part 16

2 Lab based experiment 16

2.1 Set up for the experiment 16

2.2 Detection Equipment tested 17

2.3 Measurement results on dead fishes 18

2.3.1 Effect of water thickness on the x-ray image quality 19

2.3.2 Image in 12-15 cm of water on small fishes 19

2.3.3 Detection of overlapping fishes 21

2.3.4 Imaging of fishes in 14 inches pipe 21

2.3.5 Comparison between simulation and experiment 27

2.3.6 Water variation and air bubbles 28

2.4 Image analysis 29

2.5 Summary of the lab-based trials 30

2.6 Further improvement for a field utilisation 32

3 References: 33

APPENDICES

[List appendices here]

Summary of the results

This rapport documents the possibility of using X-ray imaging as a method for detecting and counting fish in a fish counting system. The purpose of the research was to investigate and document the potential of x-ray since other techniques were hampered by the water level and turbidity in the pipes and x-ray has greater penetrating power to deal with this. X-ray has also the potential to distinguish between several overlapping fishes in the pipe and as a consequence should offer a better precision on the biomass estimation.

The laboratory results show that it is possible to detect small to large fishes (800-5 000 grams) in small to large amount of water (15 cm to 35 cm tube diameter) at a speed of at least 1 meters per second with a high spatial resolution (1 mm) and a rather compact and low cost set up. Higher speed could be achieved at the expense of a lower spatial resolution. Given the large size of the fishes that have to be detected, multiplying the spatial resolution by a factor of 2 to 4 will not affect too much the image quality. It has also been verified that imaging the fishes bones, allowed detecting overlapping fishes (2 to 4) even when a large amount of water is used. This is a consequence of the similar x-ray attenuation of fish muscle and water. Typical application could be pumping of smolt to the production pens or counting of large fishes before slaughtering.

The following system parameters have been characterised using simulation models and preliminary lab-based trials

-spatial resolution: Both the geometry of the system, the source size and the pixel size should allow a transversal resolution (perpendicular to the tube) of approximately 1 to 5 mm.

-Integration time: With a fish speed of 2 m/s, 1 ms allows a longitudinal resolution of 2 mm, which is enough to detect fishes which are several cm long. For small fishes in 15 cm of water, 1 ms gives also an acceptable signal to noise ratio.

-Contrast between fish bone and fishes: This value is approximately equivalent to the contrast between bone and water as water and muscle have approximately the same density and x-ray attenuation properties. With our simulation model a value of 0.15 for 4 cm thick fishes and 0.35 for 10 cm thick fishes were calculated in tubes with diameter of 20 cm and 30 cm respectively (contrast calculated as $(SNR_{water} - SNR_{fish})/SNR_{water}$). Values ranging between 0.2 and 1.6 have been measured on smaller fishes in small amount of water.

-X-ray effect and voltage: Voltages between 90 and 160 kV and filament current of at least 5 mA (around 500 W) had to be used to obtain a reasonable signal to noise ratio. This high power is mainly due to the attenuation in a high volume of water and the speed at which the fish have to be detected. However, given the gain that could be achieved using time averaging, and better detector, it should be possible to decrease the power by a factor of two. The voltage however has to be high enough, at least 90 kV, to allow enough x-ray photon to cross the water volume in a short time slot. To give an order of magnitude, 80 kV is the minimum source voltage that is used when performing X-ray CT on human thorax. In the simulations, almost no x-ray photons manage to cross the tube within the integration time if they had energies less that 30 keV.

-Interfering parameters – the effect of air bubbles: This effect is important and has not been fully evaluated since it is has been difficult to document it precisely enough. The only way to assess it correctly would be though tests on a (pseudo) real system. However both simulation and experimental trials show that it can be compensated for to a certain extent. The effect of a simulated volume of air between 0 and 10 % randomly distributed in the total volume of water still allows distinguishing a fish from the water.

-Imaging features of interests for the detection of fishes

The bones of the fishes are obviously the features of choice for the detection of one or several overlapping fishes. The other parameter that could have a real impact is the swim bladder, which gave a very strong contribution to the contrast. It is a feature to look for in the image in combination with the dorsal bones. The refraction effect at the edge of the fishes could also help in identifying and defining further the position of fishes, especially when imaging with small amount of water.

-Evaluation of costs:

Based on the study done so far, the production cost of an x-ray prototype has been evaluated to start around 37000 euros. This would comprise:

- An x-ray source (50-160 kV, 15 mA) with a cost of 10000-20000 euros depending on the models
- x-ray line array detector and electronic: >10000 euros. The price is very dependent on the detector type and the application. It should be a custom solution adapted to the geometry of a counting pipe
- Shielding: 12000 euros
- Data acquisition electronic and software: 5000 euros

1 Simulation of a x-ray based fish counting system

1.1 Description of the simulation set up

The illumination of a fish counting system by x-ray and the detection of the attenuated X-ray beam by a scintillator/photodiode system has been simulated using Matlab. Since the main purpose of the simulations was to verify feasibility with respect to resolution, speed and signal-to-noise levels, the following simplifications have been made:

- Rectangular cross sections of the counting system and the fish.
- Only attenuation of x-ray along the line joining the point source and the detector is taken into account (it means that attenuation of scattered photons, resulting in some blurring of the image, are not taken into account).
- Only the photodiode and a load resistor are taken into account in the calculation. The effect of front end amplifier, DAC etc which may amount to 10-20% of the final result has not been taken into account.

1.1.1 Interaction of x-ray with matter and material parameters

X-ray photons may travel a long distance before they interact with matter and terminate their history. Therefore one need to consider the number of photon that are removed from a beam penetrating a material. The Beer-Lambert-law is used to describe the attenuation of a narrow and parallel beam of mono-energetic photons going through a thin slab of material with thickness d and attenuation coefficient μ:

$$I = I_o e^{-\mu d}$$

The attenuation coefficient is composed additively of contribution from several independent interaction mechanisms: the photoelectric effect, the Compton scattering effect and the Rayleigh scattering effect. Those effects represent probabilities that a photon undergo an interaction with the material. With photo electric effect the photon is absorbed in material and disappear from the beam. It is therefore the mechanism that contributes most efficiently to the formation of the x-ray image in a pure transmission configuration. The dependence to the density, energy, structure is different for the three effects. For photo electric effect, interaction decreases very fast with energy and is dominant for material with high density. In water, the photo electric effect becomes the less dominant effect after 50 keV. For the fish counting application, the beam energy has to be high enough such that enough photon crosses the fish tube and contributes to the signal in a short time slot. At the same time, the energy has to be low enough such that the main interaction effect in the fish is the photoelectric one. This means that the application is demanding in term of source power and detector sensitivity. The Figure 1 shows the total attenuation coefficients of muscles, bone and water over the 1 to 100 keV energy range. Those coefficients are taken from the NIST website: http://physics.nist.gov/PhysRefData/XrayMassCoef/tab4.html and corresponds to human attenuation properties. As expected, muscle and water have nearly equals X-ray attenuation properties over the whole energy range. The main contribution to the image is thus expected to come from bones.

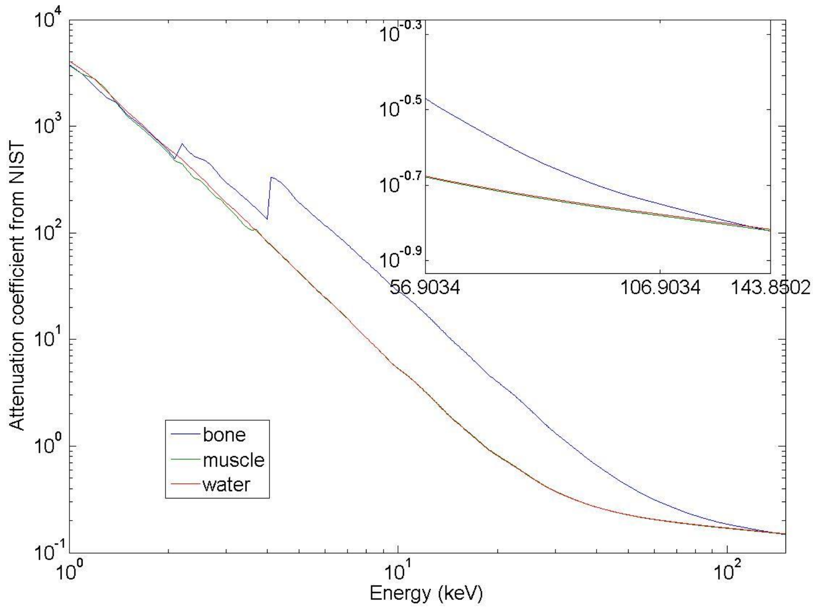

Figure 1: Attenuation coefficient (cm^2/g) as a function of X-ray energy for muscle (density:1.05 g/cm^3), bone (1 .92 g/cm^3) and water (1 g/cm^3)

1.1.2 Simulation set up

The set up is described in . Four cases were simulated. The first three are described in figure 2:

- Case a): X-rays are attenuated by one fish (bone + muscle).
- Case b): X-rays are attenuated by two fishes (bone + muscle + muscle)
- Case c): X-rays are attenuated by two fishes (bone + muscle +bone +muscle)
- Case d): X-rays are only attenuated by water.

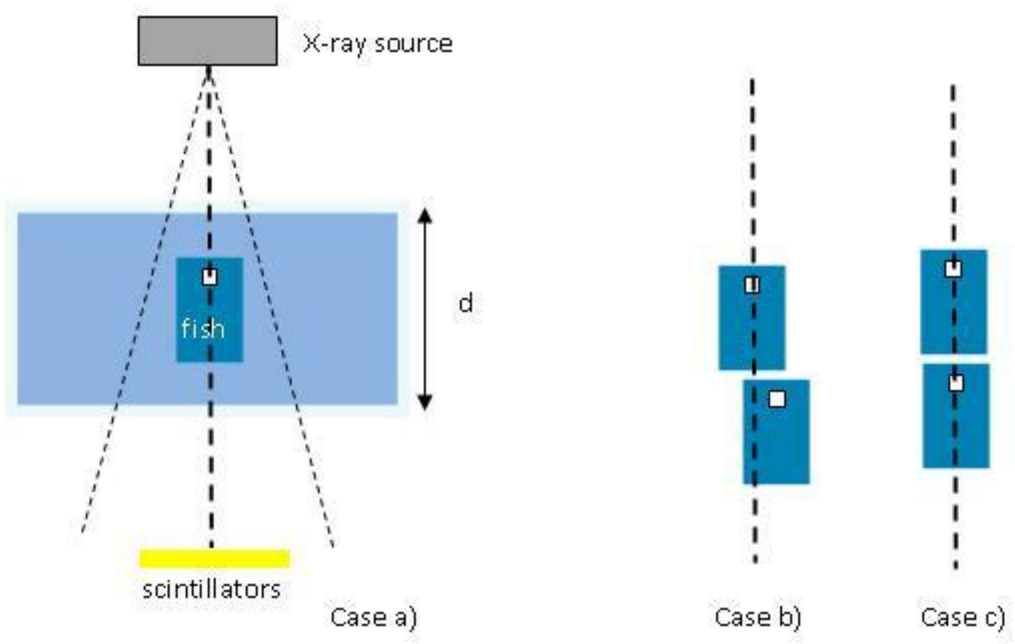

Figure 2: Set up for the simulation; Case d corresponds to water only

Simulations were done both for water with and without bubbles. For a ”tube” with a diameter of 30 cm, a source emitting X-ray within an angle of 20 grader is enough to cover the whole tube at a distance of 85 cm from the center of the tube.

1.1.3 Fotodiode response

The photodiode response was calculated as follow:

- Calculation of the X-ray spectrum
- Calculation of X-ray attenuation through the fish in the different cases.
- Calculation of the scintillator/photodiode response to the attenuated X-ray beam.

Figure 3 shows an example of a X-ray spectrum calculated using a software called “SpecKalk” (http://www.icr.ac.uk/research/research_sections/physics/3544.shtml). This software allows calculating X-ray spectra from tungsten anode X-ray tube. The maximum voltage, primary filtering and angle of anode/emission can be chosen by the user.

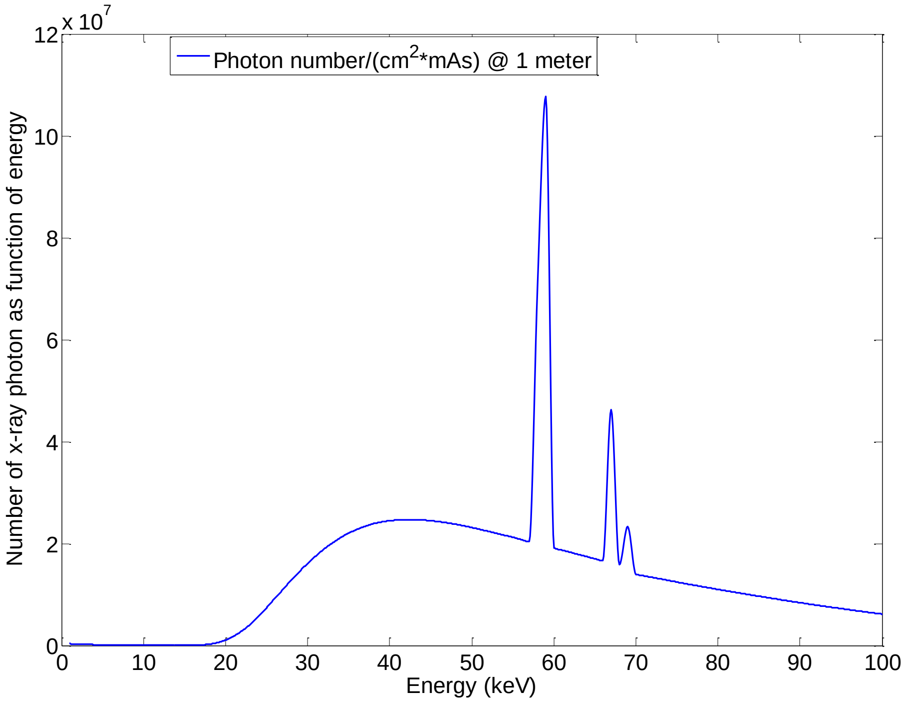

Figure 3: Wolfram Source fluence with Mo and Al filter. Voltage = 130 kVp. Angle of emission 20 deg

The calculation of the X-ray attenuation from the X-ray point source to the photodiode pixel was done using the Beer-Lambert law and the coefficients of figure 1. The bubbles were taken into account by assuming that the corresponding total air length seen by X-ray corresponds to 0 to 10 % of the tube diameter, i.e in the case where there is only water, the water length seen by X-ray was varied between 27 and 30 cm .
The scintillator-photodiode response was calculated using a model from the literature [Kalivas]. Only GOS scintillator, (Gd_2O_2S) was tested, other scintillator may also be suitable. The photodiode characteristics were taken from Hamamatsu. The parameters used for the simulations are given in the following table:

Table 1: fish parameters used for the simulation

Tube diameter	Fish length	Fish height	Bone thickness	Equivalent air thickness	Fish speed
30 cm	40 cm	10 cm	0.5 cm	0-3 cm	2 m/s
20 cm	15 cm	4 cm	0.2 cm	-	2 m/s

The integration time was chosen equal to 1 ms.

1.2 Identification of optimal source voltage

Figure 4 and 5 show respectively the current and the signal to noise ratio in the photodiode for the four cases shown in figure 2. Both dark signal at 10 mV, Johnson noise of the load resistor and shot noise (assumed to be Poisson distributed) were taken into account. The figure 6, shows the contrast with water. The contrast was defined as:

$$\frac{SNR_{water} - SNR_{case}}{SNR_{case}}$$

The calculations are done for several X-ray tube voltages (90 to 130 kV). It can be seen that even though the current amplitude and SNR are lower for the 90 keV (less transmission @ lower energy), the contrast with water is higher (the attenuation cross section contrast between water and bone decreases with the energy, cf figure 1). The signal obtained without any matter gave a calculated current a little above 1 nA when using a 120 keV source, 6 mm Al filtration and 1 mA. The specifications of Hamamatsu using “the same” tube characteristics being between 2 to 5 nA depending on the scintillator used.

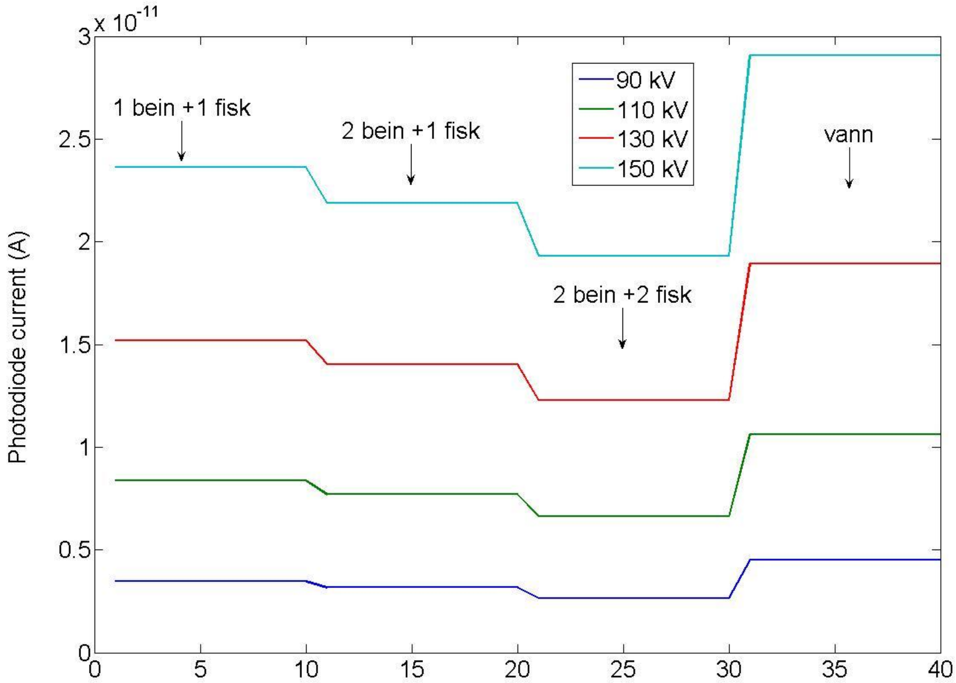

Figure 4: Photodiode current without bubbles for the 4 cases.

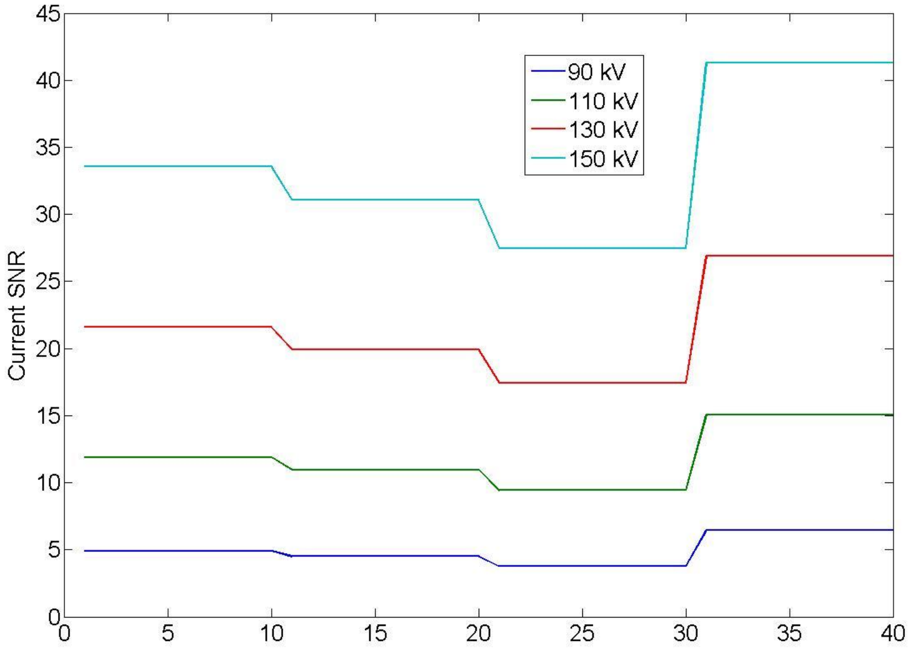

Figure 5: SNR (I mean/I noise) without bubbles for the 4 cases.

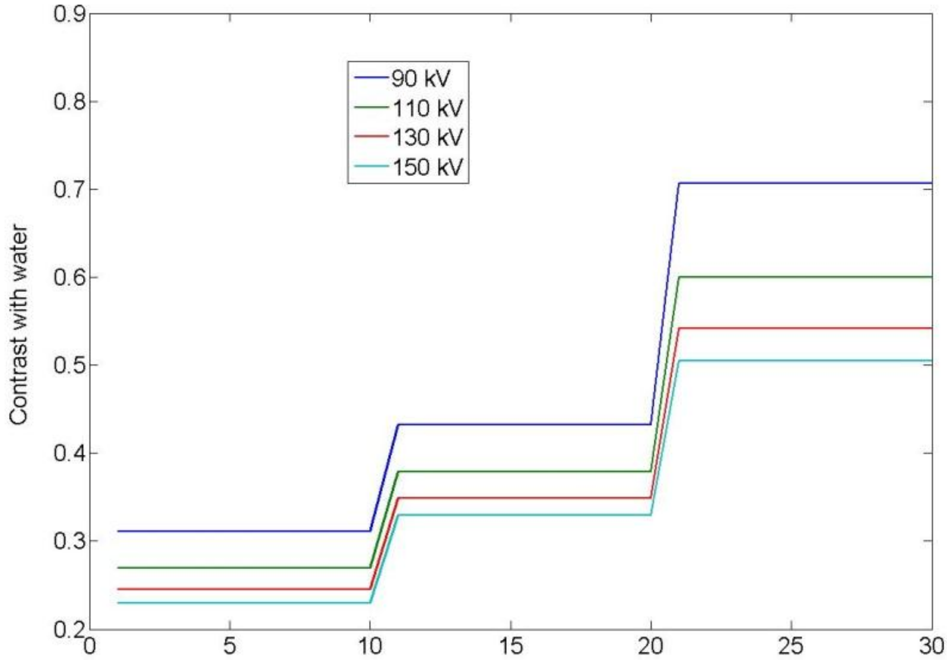

Figure 6: Contrast of the three first cases with water: (SNR water – SNR case)/SNR case

Those figures show that a reasonable voltage, in term of contrast and signal to noise ratio, should lie in the 90 – 110 keV range but that possibly higher current level has to be used to increase the SNR.

1.3 Effect of air bubbles

Figure 7 shows a simulation of the noise introduced to the signal when air bubbles are introduced . For each case, a set of hundred effective air lengths chosen randomly between 0 and 3 cm were calculated to mimic the effect of bubbles, and the photodiode response was calculated. The figure shows the response when using 110 keV and 5 mA. The contrast between water only and one or two fishes is still acceptable, but differentiating two overlapping fishes from one fish is more difficult. The effect of air plays an important role in the detection scheme, so a better knowledge of the bubble distribution is required.

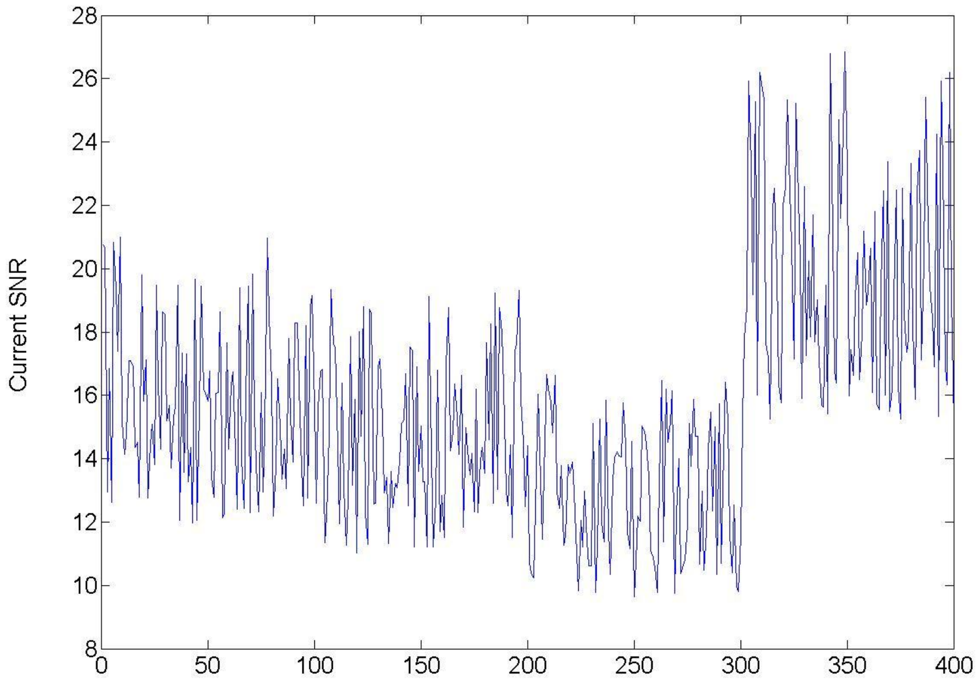

Figure 7: Effect of air buble on the SNR for kV= 110 for the 4 cases .

1.4 Effect of the scintillator thickness on contrast and SNR

Figure 8 shows the SNR calculated using different thickness of a commercial scintillator (UFC) and parameters from a commercial source @ 90 keV (90 keV, 15 mA, 40 degree angle emission). The scintillator has better optical properties (UFC) than conventional GOS. The contrast with water is shown in figure 9. The source emits with an angle of 40 degrees. The higher signal to noise ratio is obtained for the 300-400 µm thick scintillator (see figure 8), while a better contrast with water is obtained for the 100 µm thick scintillator (see figure 9). A possible explanation could come from the fact that as the scintillator thickness increases, the optical signal generated from the low energy x-ray photon, i.e. those that contribute most to the contrast, are more attenuated (as it is generated in the top of the scintillator). The fact that the contrast increase as the scintillator thickness decrease is due to the fact that for a scintillator with small thickness, the x-ray photon with high energy will be less attenuated that x-ray photon with low energy. A scintillator with low thickness will give more statistical weight to low energy photon, i.e. to the photon that bears most contrast information, while it will give less weight to photon that contributes most to noise, i.e. photons with high energy.

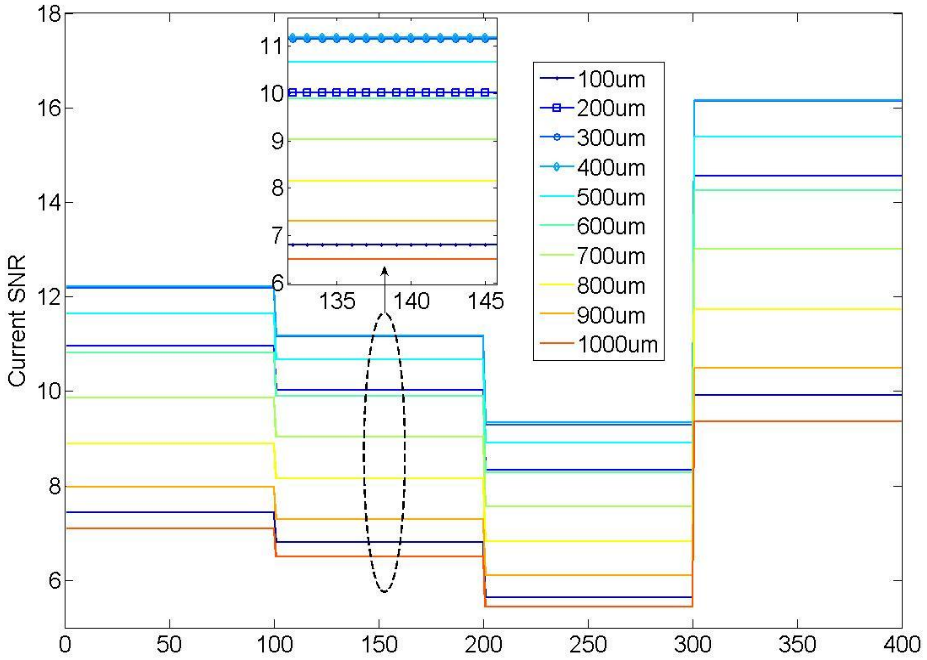

Figure 8: Current SNR ion the 4 cases obtained using UFC and a 90 keV, 15 mA, 40 degrees source for different scintillator thicknesses

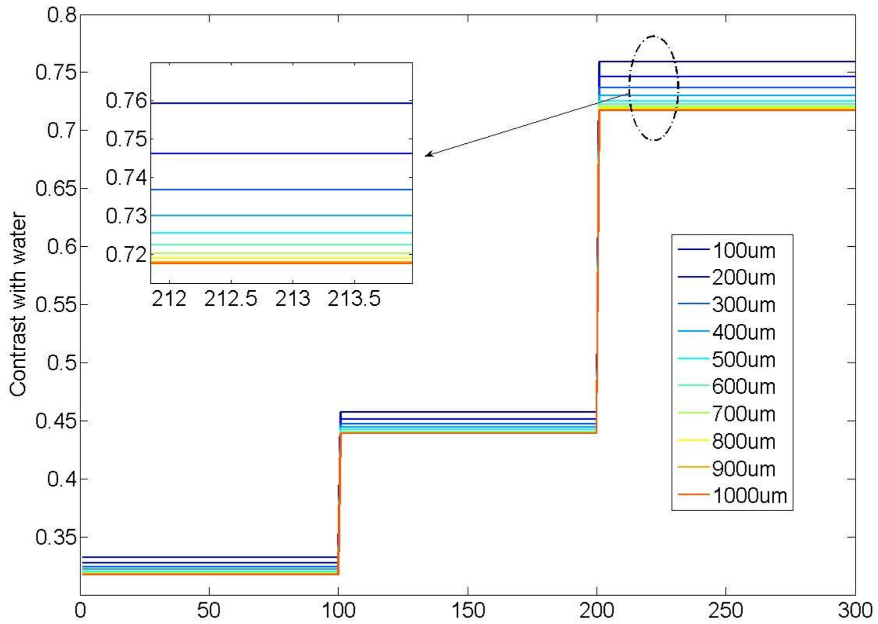

Figure 9: Contrast with water for the cases a) to c) using UFC and a 90 keV, 15 mA, 40 degrees source for different scintillator thicknesses

A thickness between 100 and 400 µm seems thus to be optimal both in term of contrast to noise ratio with water @ 90 keV.
Higher value for the current and SNR are obtained usually by pixelating the scintillator and coating them by a good reflector (TiO_2). This is not taken into account in the simulation which gives thus a lower estimate of the measured signal. It is possible to reach a 50 % enhancement in the total amount of optical photon detected using coated and pixelated scintillator, meaning a decrease by half of the current needed to perform the measurement. This lowers the price of the source and the need for shielding.

As mentioned before, the energy are integrated in an indirect conversion detector, the physical contrast is “averaged” over the energy range that is used by the x-ray system, and thus the contrast measured is significantly lower than the difference in attenuation coefficient of interest, i.e. between bones and water. To approach the optimal contrast, the energy gain of the x-ray system can be modified or corrected by energy weighting function. Energy weighting function applied to the spectrum, before summation of the detected energies can improve drastically the contrast between a background and the object to detect. Figure 10 shows examples of an optimal weighting function for different imaging tasks. Those were calculated for the purpose of bones imaging in water (bones thickness 100 um (blue), 1 mm (green) and 1 cm (red)) in a background of soft tissues or water.

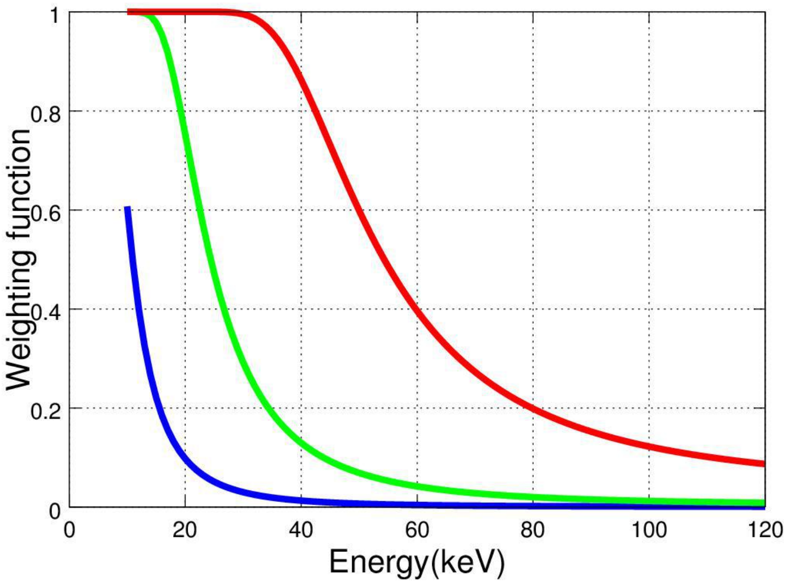

Figure 10: Ideal weighting function for imaging of bones in soft tissues or water; weighting function for 100 um bones (blue), 1 mm bones (green) and 1 cm bones (red)

For the all the cases, the weight is put on low energy region. This illustrates that when relatively increasing the photon flux in this energy region, by any means (adapting the spectral shape of the source, using adaptive filter changing the thickness or the type of the scintillator) will improve the contrast between bones and water.

1.5 Simulation on small fishes

Imaging of a small fish with dimensions given in the table 1 has also been simulated using a scintillator with thickness 400 µm. A voltage of 90 kV and current of 15 mA has been used as previously. The SNR is much higher (around 100) in this case because X-rays are crossing less matter. The contrast with water is however smaller as can be seen on figure 10.

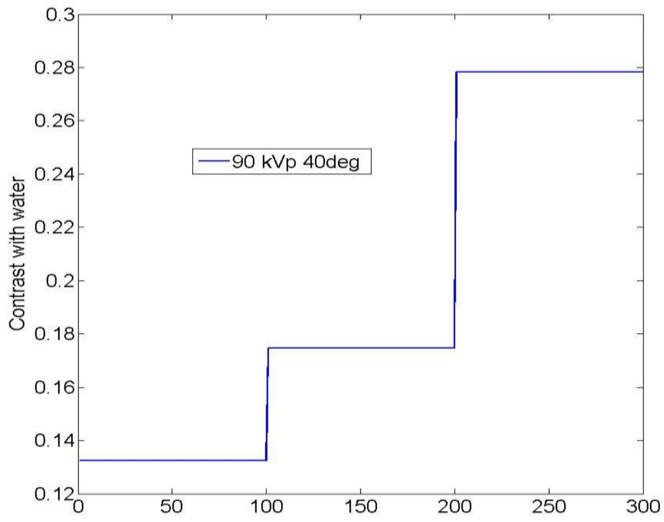

Figure 11: Contrast with water in the cases a) to c) obtained with a smaller fish

1.6 Spatial resolution

The geometrical configuration used in this simulation give a magnification of approximately 1.25 and a geometrical blurring inferior to 200 µm depending of the source size. The pixel size used in the simulation equals 1.5*1.5 mm, meaning that an estimate of the smallest detectable detail lie around 1 mm. Scattering of X-ray will also contribute to the deterioration of the image quality, but this effect is more difficult to quantify, since it would require a simulation of the photon transport in the complete geometry.

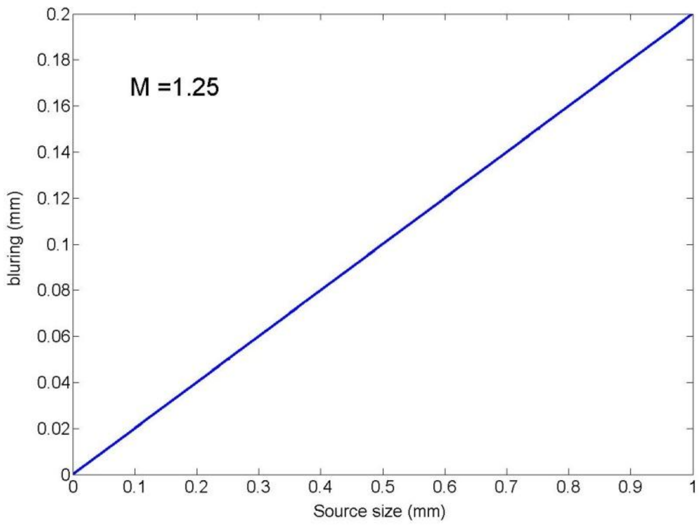

Figure 12: Blurring as function of the source size

1.7 Summary of the simulation part

In this part we have evaluated numerically the expected contrast and of bone with water and the signal to noise ratio for a typical fish counting situation. Parameters like the scintillator thickness, the source voltage effect of air bubbles have been evaluated. The whole imaging system has to be optimized for a specific imaging task; i.e. detects one or several bones in a large amount of water. The thickness and type of the scintillator can be optimized further to increase the contrast, or contrast to noise ratio. The spectral shape of the source is also an important point to optimize. Sources that provide a high flux in the lower part of the energy windows (50-100 keV) should be prioritized, though it is difficult to adapt this in practise.

2 Lab based experiment

Based on the simulations results a series of experiment have been performed using dead fishes being scanned over a scintillator photodiode array and x-ray cameras for different x-ray energies and current. Two configurations have been tested:

- Imaging in a small amount of water with very small and medium fishes
- Imaging in a full 14 inches pipe with medium to large fishes

2.1 Set up for the experiment

The experimental set up is presented on Figure 13 and Figure 14. When working with small fishes, < 1kg, a small container was used and filled with different amount of water. One or several fishes could then be placed in the container which could then be scanned over the line array photodiode. With longer fishes, > 4 kg the whole fishes, or pieces of fishes were fixed to a rope and pulled inside the container, or the whole container was scanned over the x-ray detectors. An open container, not shown on the figure, has also been used for the test with the larger fishes.

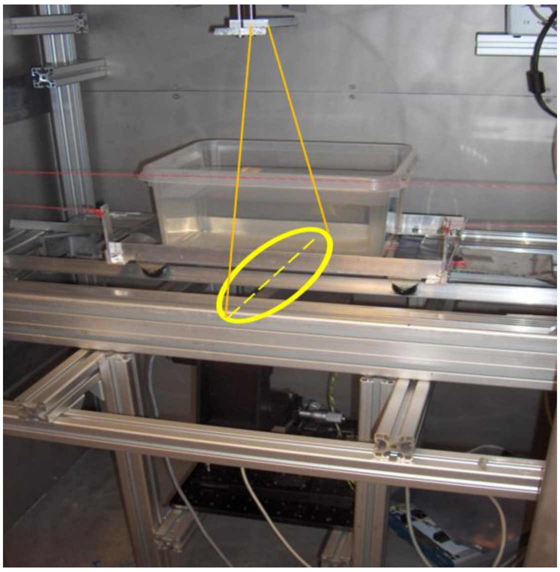

Figure 13: Experiment setup built for the measurement on small fishes. The location of the diode array is symbolized by a yellow dashed line

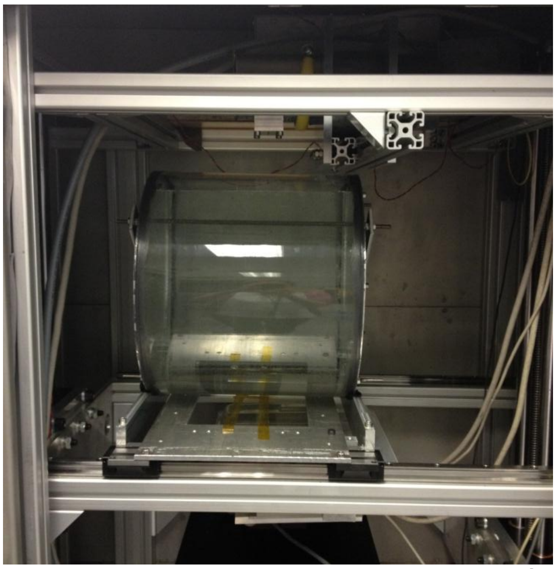

Figure 14: Experiment setup built for the measurement on large fishes.

The amount of water that could be used ranges from 15 cm max in the setup of Figure 13 to 35 cm maximum in the setup of Figure 14. 10 to 25 cm long fishes could be measured in setup of Figure 13 while part of fishes up to 5 kilos (80-90 cm long) could be used in the setup of Figure 14.

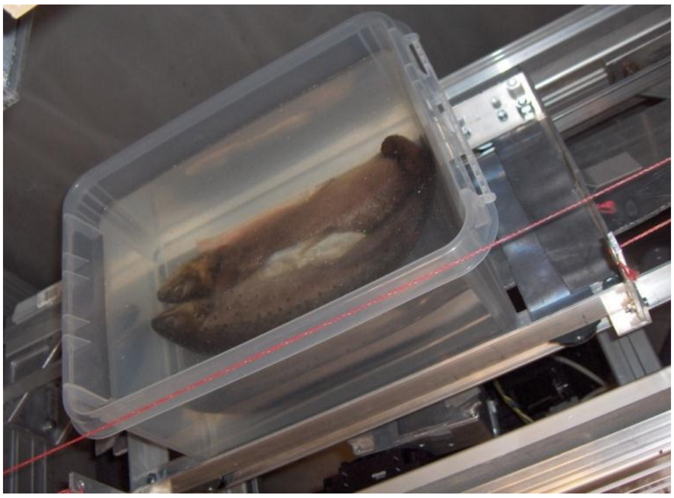

Figure 15: Set up for imaging two overlapping fishes

The distance between the source and the water holder, d, ranges from 50 to 80 cm while the distance between the holder and the detector, z, was varied between 5 cm to 10 cm. With this geometry, the magnification was close to 1. The x-ray source had a focal spot size of 3 mm, which is smaller than most of the detail that we are interested in seeing in the fish. The magnification has also an impact on the blurring due to the finite size of the focal spot size. The result is a loss of sharpness in the image. The edge blurring is given by z/d. It increases as the magnification increases. Given our low magnification, it could also be neglected in our case. The source could be driven up to 1600 W continuously. For 100 keV, a current of 10 mA can then be reached, which is a reasonable value. By comparison, medical sources used for CT reaches temporarily several hundreds of mA at the same voltage.

2.2 Detection Equipment tested

The tests have been performed using low cost detectors from Hamamatsu (see Figure 16 and Figure 17 b)) and x-scan imaging (Figure 17 a). The photodiode array is a line array CMOS photodiode covered by a scintillator sheets made of Gd2O2S:Tb. The thickness of the sheet amounts to 300 um. The photodiode are combined with a signal processing unit made by CMOS process. It incorporates a timing generator, shift register, charge amplifier array, clamp and hold circuit. A driver circuit was used to control the two sensors. Using two signals, a clock and integrating signals, the integration time of the sensors can be tuned from some microseconds to several milliseconds. The circuit are thus fast enough to allow the acquisition of enough line scans per fish (> 10 lines) for fish speed up to 2 meter/s. Those small sensors are well adapted for mounting on non planar geometry. The x-ray cameras have been rented for the tests on the large pipes. The pixels resolution ranges from 48 um to 400-800 um.

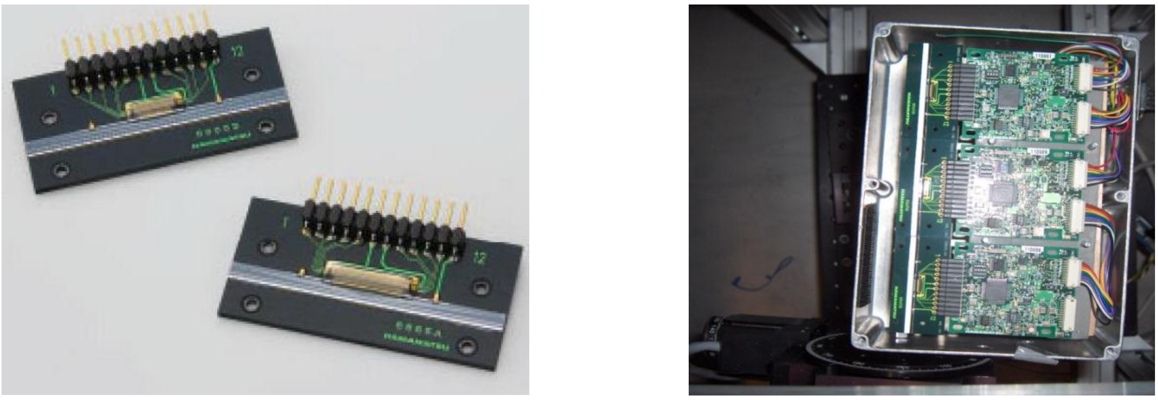

Figure 16: Photodiode array from Hamamatsu a; line sensors in b) with controller

Line sensors have been designed by aligning several sensors side by side. The whole sensor was controlled by a LabView application which controlled the integration time and rate and allow the x-ray signal acquisition. The data were then processed using Matlab routines.

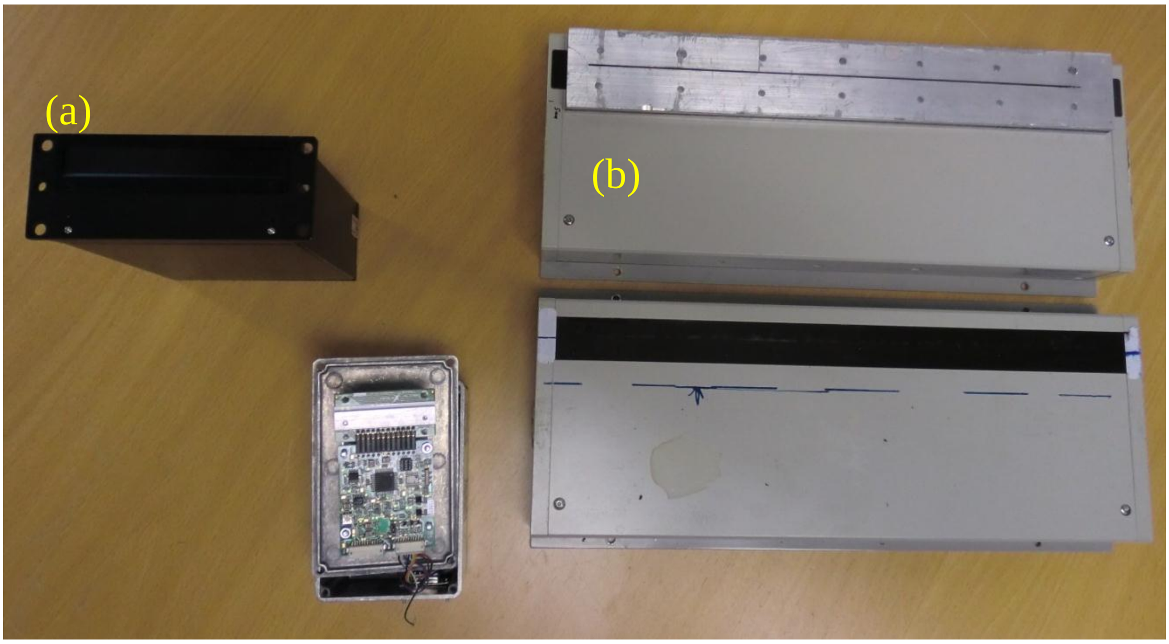

Figure 17: X-ray cameras used for the tests with the smolt (a) and for the measurements on the large pipe (b, c)

The cameras used for the tests in the large pipe could be controlled using traditional frame grabber and software.

2.3 Measurement results on dead fishes

Images were taken with different amount of waters using different voltages and current. Some results are presented in the following paragraphs.

2.3.1 Effect of water thickness on the x-ray image quality

Water and tissue have approximately the same density and attenuation coefficient, a larger amount of water lower the contrast difference between the flesh of the fish and water. This can clearly be seen on Figure 18 and Figure 19 where, the tissue almost disappear as the amount of water goes from 2 cm to 12 cm @ around 53 keV. When the amount of water is of the order of the fish thickness, the most visible features in the image are the bones, which have the highest density and attenuation coefficient.

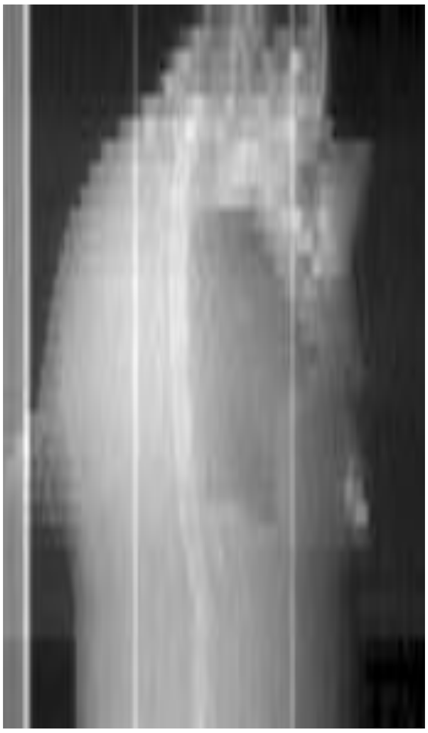

Figure 18: 53 keV, 1.3 mA, 2 cm water

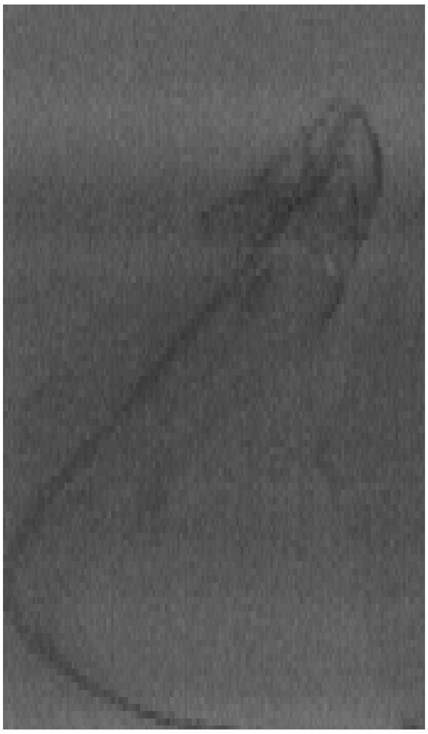

Figure 19: 55 keV, 6 mA, 12 cm water

2.3.2 Image in 12-15 cm of water on small fishes

The fishes used in the experiment were 30 cm long trout. The dorsal bone size thickness was approximately equal to 7 mm. A fix amount of water was used while varying the voltage and current intensity such that the detectors are close to saturation for each couple of value (kV, I). The focal spot size was set to 1 mm. The x-ray beam was apertured both on the source size and on the detector size. This has been shown to be very important for the quality of the image. An aperture of quality on the source size allows obtaining a well defined fan beam, and in principle allowing illuminating only the detector region. This reduces the radiation dose to the surrounding and allows avoiding also illuminating region that will not contribute to the image creation. However, due to Rayleigh and Compton scattering, the fan beam geometry get degraded in water and some photons not having gone through the fish may reach the detector through scattering. To avoid this, one or several aperture should also be placed in front of the detector to filter part of the scattered photon beam. Another solution is to use a large air gap between the detector and the pipe. In our experiment, we used home made slit made from lead and aluminium. The slit were positioned in front of the detector. A set of linear translation and rotation stages were used to align the line detector with the fan beam. Examples of x-ray images taken of a scene with two fishes are shown on Figure 20. The source voltage ranges from 55 to 90 keV while the current ranges from 10 to 7 mA. A general comment is that the fish bone structure can clearly be seen in all the images. The contrast between bone and water is still good even for 90 keV even if at that high energy, the photoelectric cross section is low. The structure in the head, the vertebra, the fin and even the tail can be distinguished easily for almost all the kV setting. The flesh is also visible, especially the contour. This can also clearly be seen on the processed images and come from refraction effects: x-rays are refracted as conventional electromagnetic waves. This effect is seen close to boundaries between materials with different densities where x-ray are bent because of the difference in refractive index. Due to the fact that at x-ray energies the refractive index is smaller than 1, the x-ray are refracted away from the denser part, i.e. away from fish muscles; close to the boundary between fish and water, the signal strength of the denser side will be weaker than on the other side. Example can be seen on Figure 20 c), at the boundaries between the dorsal region of the fishes and water.

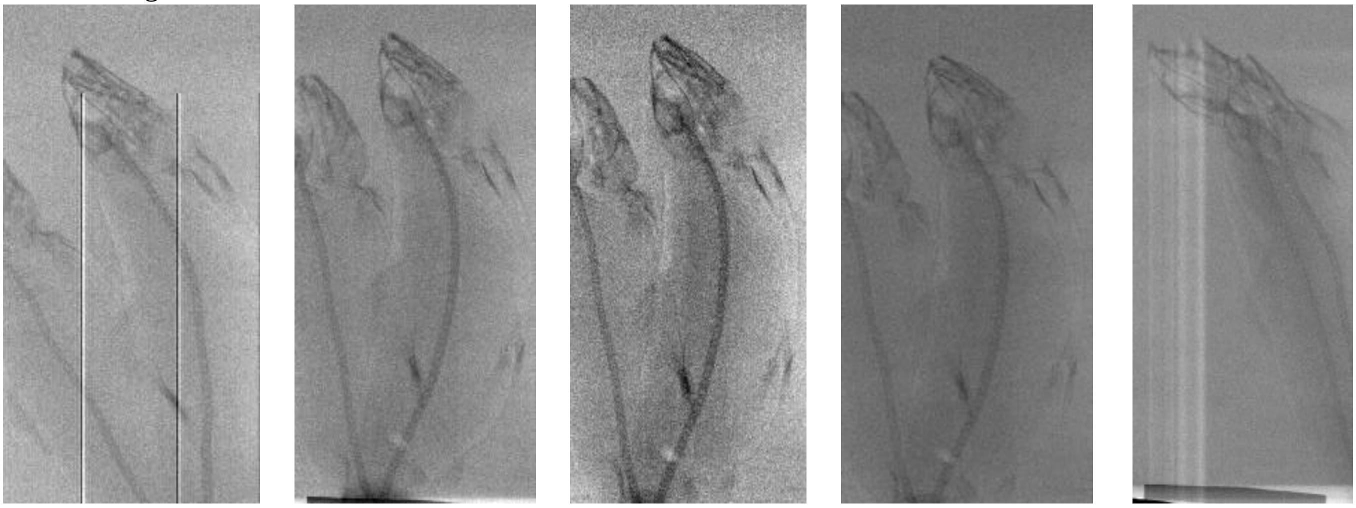

Figure 20: X-ray acquisition for voltage ranging for a couple (kV, mA) equals to (55, 10) (a), (60,10) (b), (70,9) (c), (80,8) (d) and (90,7) (e) for 12 cm of water

A set of image was also taken using a large focus of 3 mm. This option of the source offers more power, but the image quality should suffer from blurring due to the projection of the finite size source onto the image plan. As can be seen on Figure **21**, the blurring effect did not degrade the image quality and the contrast is still very good. Note that the power has been increased, which obviously help in increasing the SNR and could have help in compensating for a pert of contrast

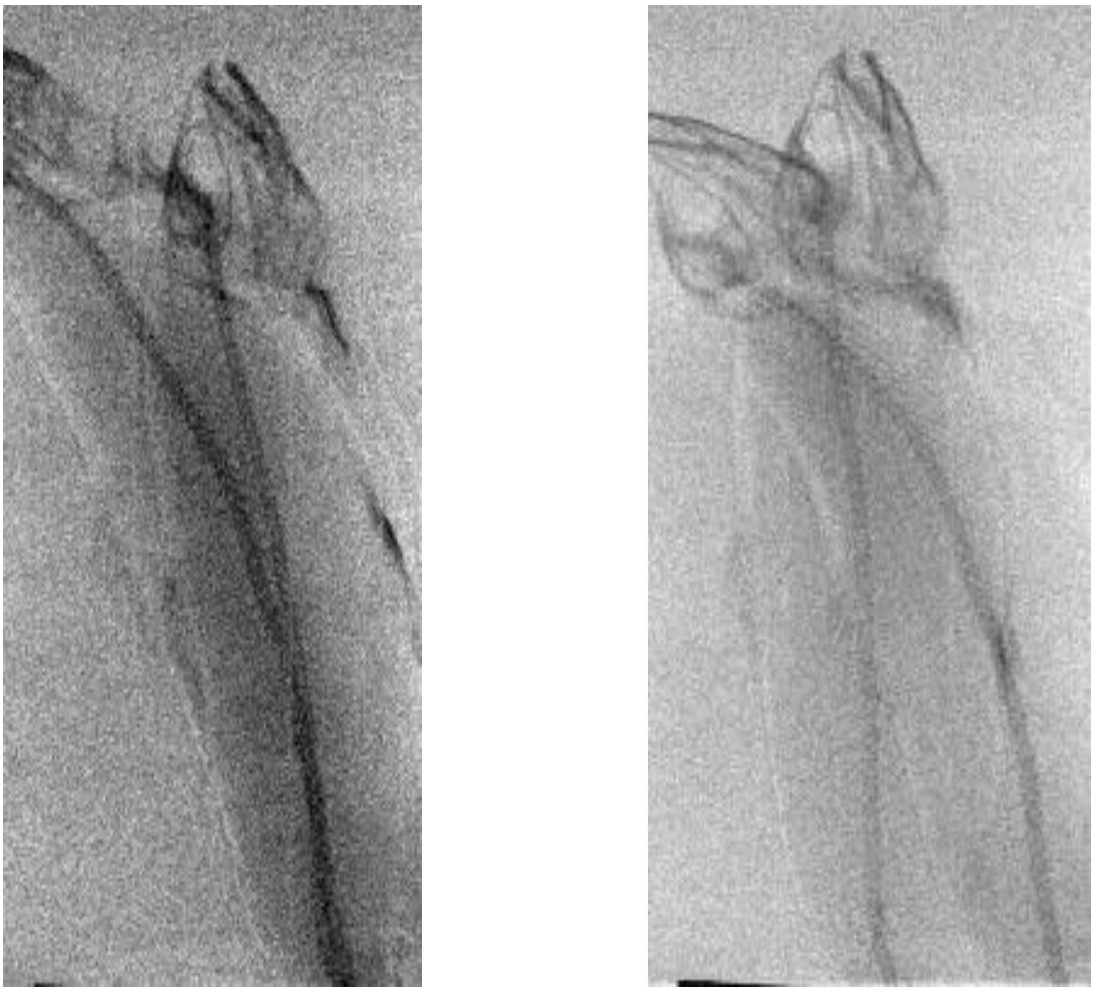

Figure 21: **Measurements at 55 kV, 10 mA, taken with a large focal spot size**

2.3.3 Detection of overlapping fishes

In those very good conditions of measurement there are no problems in distinguishing two fishes that overlap. This should nearly be independent of the number of fishes that overlap. This is again due to the similar attenuation of water and flesh. Assimilating flesh and water as the same entity in the image, an automatic identification of fishes reduces to the identification of the fish bones. Two or several fishes that overlapped will be identified as two or several fish dorsal bone that crosses. As these are rather small entities, the probability that these two perfectly overlap over the whole fish length is small.

2.3.4 Imaging of fishes in 14 inches pipe

In those series of experiments, fishes with different weight have been tested. In the following, results for a 5 kg fish, 3 kg fishes and 0.8 kg fishes are presented. The experiment set up is shown on Figure 14. The experiment was done as follow:

1. Experiment with 800 grams fishes: five fishes were sewn together in order to simulate a cluster of fishes in the pipe (Figure 22 and Figure 23)
2. Experiment with 3 kg fishes: Different part of the fishes were cut and inserted in the pipe. A small balloon was inserted in one of the fish, to simulate a swim bladder (Figure 24 and Figure 25)..

3. Experiment with 5 kg fish (Figure 26 and Figure 27): The fish was cut and only the central part was inserted in the pipe; here also a balloon was inserted in the fish to simulate the effect of a swim bladder on the x-ray image

A general comment is that higher voltage were needed compare to the last series of experiment to be able to have a high enough signal to noise ratio. The cause is the larger amount of water which attenuates much more the x-ray beam. Another comment is that the image quality increases with the size of the bones and thus with the size of the fishes. This is logical since larger bones will attenuate more x-ray than thinner bone, and thus contribute more to the contrast with water. The small fishes can however be seen with a good contrast. Overlapping fishes are also clearly distinguished, whether in the configuration 1 or in the configuration 2.

The swim bladder gives a very strong contribution in the image (white circular region). Its contribution to the image can be easily higher than the contribution of the bones, because of the higher difference in attenuation coefficient between air and water. However, it can easily be confounded with air bubbles. It should be a feature to track in the images in combination with the bone signatures.

The other features of interests are the contour of the fishes, caused here also by refraction effect at the edges of the fish. Those can be also be seen in these series of measurement, although will less contrast than in the experiment done in 15 cm of water.

Due to the size of the pipe, the rented x-ray cameras were used for these tests. The pixel size was equal to 400 um. The pipe could be translated at around 4cm/s. Integration time ranging from 10 ms to 45 ms were used. This amount to approximately 0.4 -2 mm per scan, and thus in average to one measurement line every mm, which is by far enough for the resolution of fishes which are several ten´s of cm long. For fishes swimming at 1-2 m/s, one scan every 1-2 mm would mean an integration time of around 1 - 2 ms. This is a factor 10-20 less than the one we have used in our experiment. The image quality obtained with the camera used in those experiments is high enough for the integration time to be reduced further and to allow the imaging of fishes at higher speed in a real application. This is particularly true for the imaging of the 5 kg fishes. 400 um large pixels offer a resolution that is not needed for the detail we are interested to see in the images (bones size ranging from 5 mm to 2- 3 cm). It is thus possible to increase further the pixel size to at least 1.6 mm. 1.6 mm would allow to record the same amount of x-ray photons at a rate 16 times higher. We can thus extrapolate from these series of experiment that with larger pixels size, imaging of fishes in 14 inches large pipe full of water with similar contrast, signal to noise ratio and good enough spatial resolution would be possible for 3 to 5 kg fish swimming at speed of at least 1 m /s and at most 3-4 m/s.

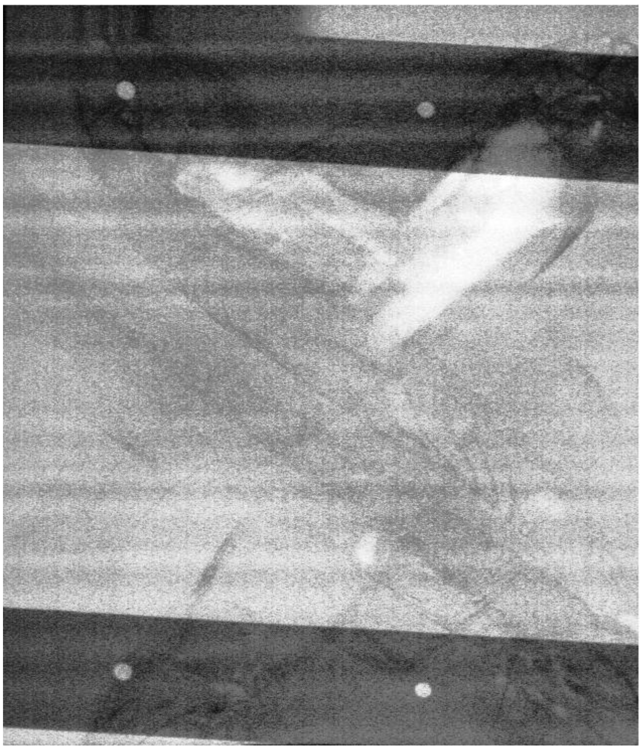

Figure 22: Fives 800 grams fishes imaged with an integration time of 10 ms and 160 kV and 6 mA

Figure 23: Fives 800 grams fishes imaged with an integration time of 45 ms at 110 keV and 10 mA

Figure 24: Four 3 kg fishes imaged with 140 keV and 6 mA; Integration time of 12 ms. Note the white contribution of the swim bladder in the image.

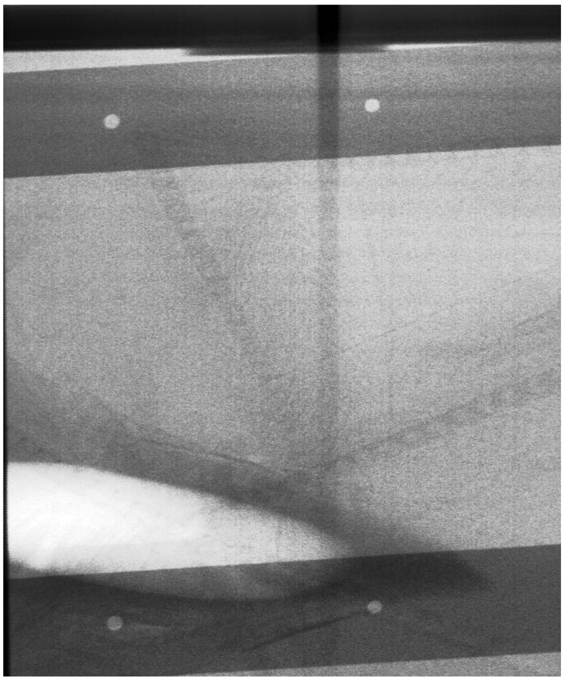

Figure 25: Four 3 kg fishes imaged with 140 keV and 6 mA; Integration time of 12 ms

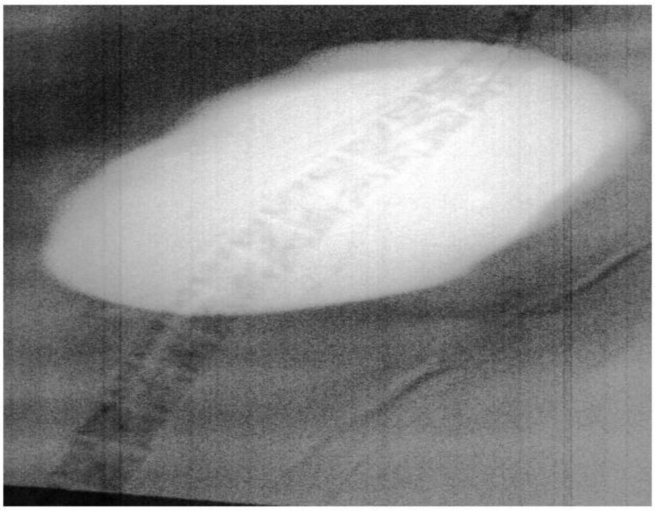

Figure 26: 5 kg fish imaged at 160 kV and 6 mA; The integration time is 10 ms

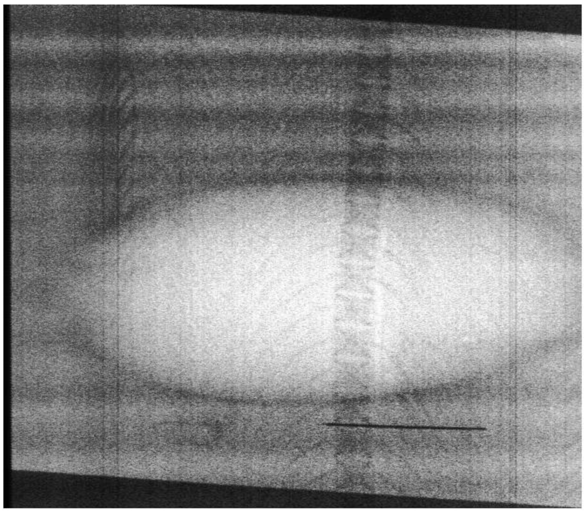

Figure 27: 5 kg fish imaged at 120 kV and 7 mA; the integration time is 10 ms

The Figure 28 to Figure 31 show extrapolated images to higher swimming speed. The original pixels data have been averaged over a square of 4 by 4 pixels to simulate 1.6 mm large pixels for the Figure 28 to Figure 30 and over a square of 6 by 6 pixels for Figure 31. The extrapolated swimming speeds are respectively 0.5 m/s and 1 m/s. These images allow appreciating what contrast and SNR to expect in a real set up. It can be seen that the larger pixels still allow to clearly seeing the 5 kg fish with a high enough resolution (Figure 30 and Figure 31). The images of the fishes of 3 kg and 0.8 kg, are of lower quality, but the contrast is still high enough for the fishes to be distinguished by eyes. Filtering, segmentation and edge detection have also been applied on all the extrapolated data, to infer the possibility to automatically detect the fish bones on real data. The swim bladders have been let apart since they gave a contrast that is high enough for their detection to be a relative easy task in practice. Examples of filtered images are shown on Figure 28 b) to Figure 31 b). While the image analysis algorithm work well for the large fish, the results are less predictable for the fishes of 3 kg and 0.8 kg. For the fishes of 0.8 kg, the segmentation algorithm did not allow to clearly separate all the fishes. Finally, note that for 5 kg fishes in Figure 30 and Figure 31, the bones contrast is higher in the swim bladders region, because there is less water to cross for the x-ray beam.

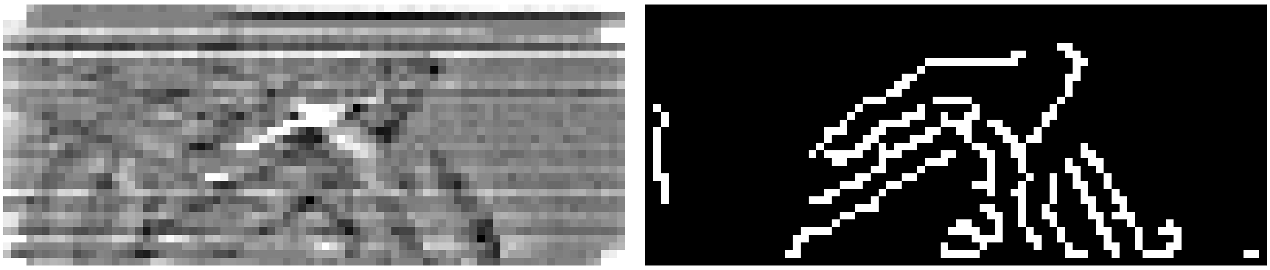

Figure 28: a) High pass filtering of the extrapolated data to fish speed of 0.5 m/s; b) Image results after application of edge detection algorithm on the extrapolated data

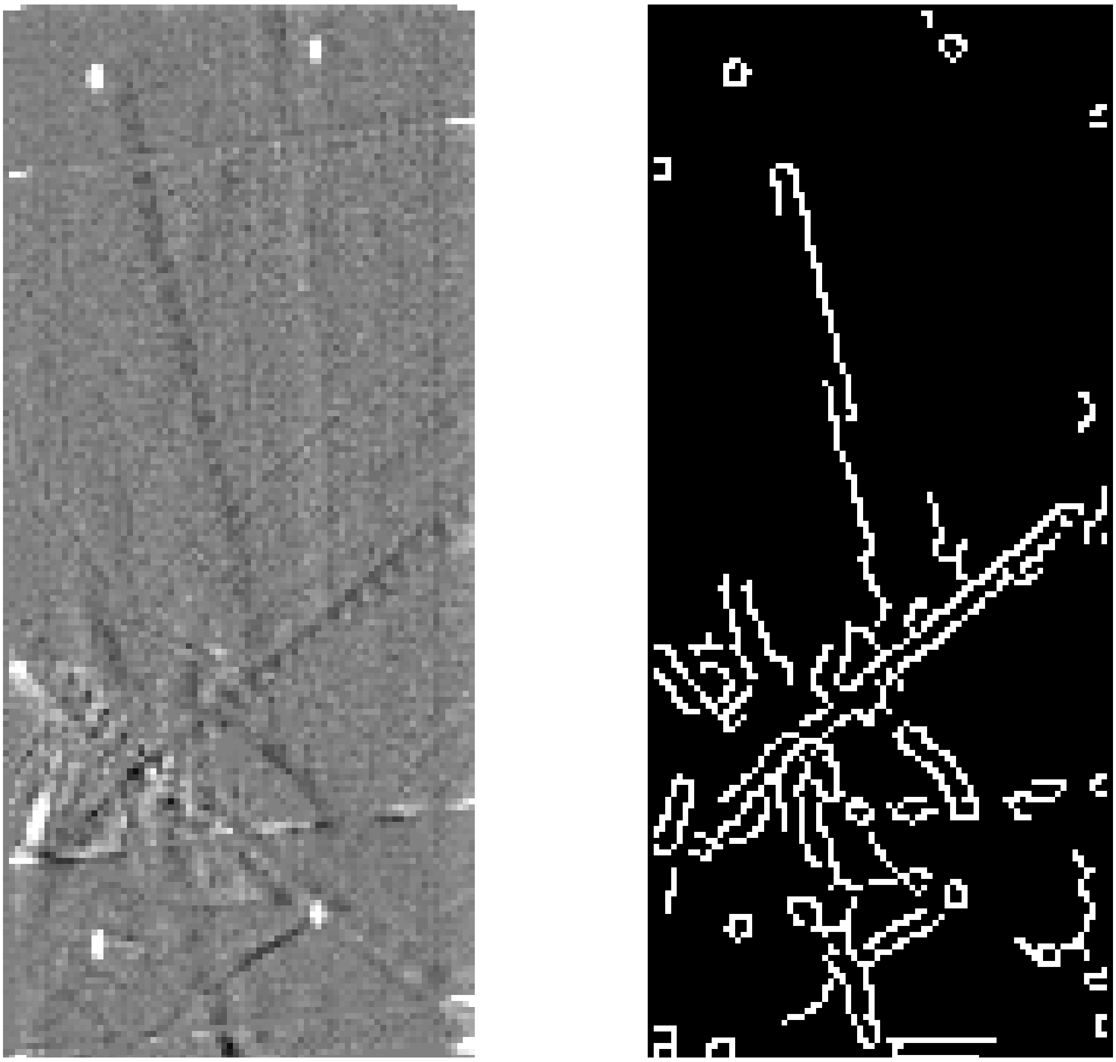

Figure 29: a) High pass filtering of the extrapolated data to fish speed of 0.5 m/s; b) Image results after

application of edge detection algorithm on the extrapolated data

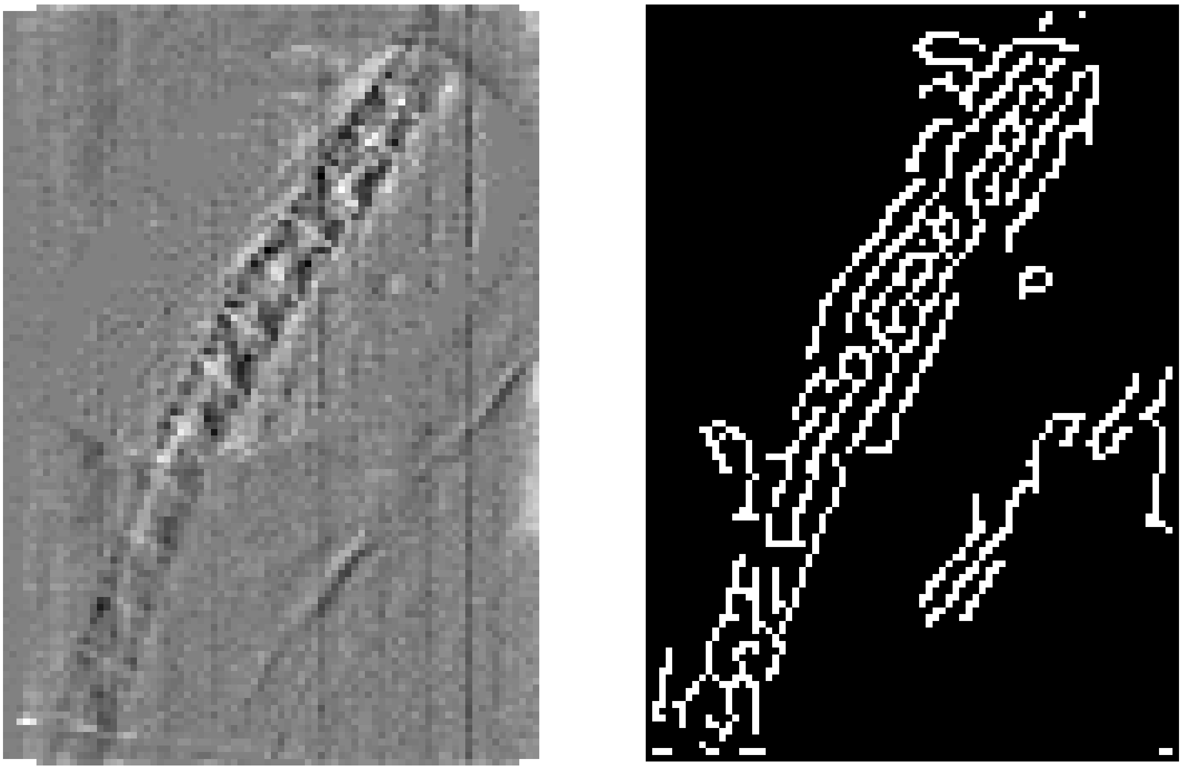

Figure 30: a) High pass filtering of the extrapolated data to fish speed of 0.5 m/s; b) Image results after application of edge detection algorithm on the extrapolated data

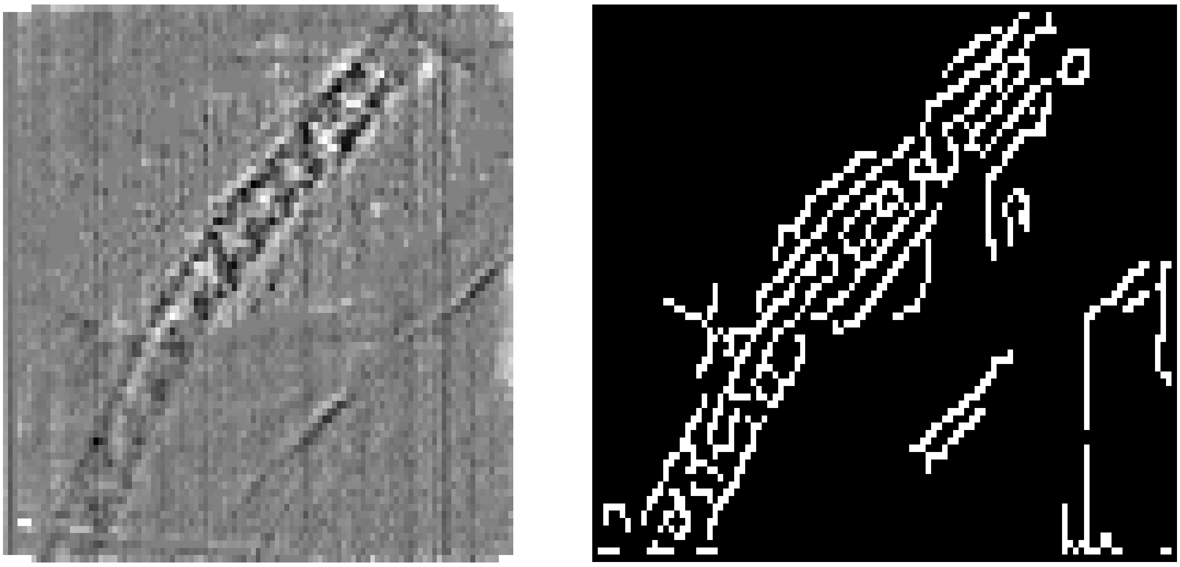

Figure 31: a) High pass filtering of the extrapolated data to fish speed of 1 m/s; b) Image results after application of edge detection algorithm on the extrapolated data

To improve the image quality further, the effect of scattered photon (Rayleigh or Compton) in the water, that strongly degrades the images quality, should be compensated for in a much better way. This is a very well known problem when attempting to take images of low density features in large object (for example in CT). We envisage the following options for increasing the SNR and contrast:

-Improve the shielding of the detector and the aperturing of the x-ray beam to decrease the impact of Rayleigh and Compton scattering. This can be achieved through the use of anti scattering grids or slits that are more adapted to the pipe set up. Ideas could be borrowed from the CT application. Use of anti-scattering grids should result in a gain in the form of increased contrast of the bone. Such grids are commonly used in CT and plain radiographic examination although there is not a consensus on their utilities.

-Use smaller pipe, or adapt the pipe shape (rectangular, elliptic) to decrease the amount of water the x-rays have to cross, while preserving the flow capacity in the tube.

2.3.5 Comparison between simulation and experiment

The contrast was evaluated on the images taken in 15 cm of water, (Figure 32 a)) to compare with the simulation results. The results of the calculated contrast for several images are shown on Figure 32 b). A simulation has been done trying to mimic the experimental condition (15 cm of water, 7 mm thick dorsal bone, 4-5 cm thick fishes) for energies ranging from 50 to 90 keV. It can be seen that the measured and calculated contrast are of the same order. In addition a simulation for 30 cm of water has been done, (Figure 33), which show that the contrast of bone with water is rather independent of the water volume. It can be shown that it is a function of both, the difference between the attenuation coefficient of water and the attenuation coefficient of bone and of the bone thickness. The SNR of course, will depend of the water amount, since a higher water volume means higher x-ray attenuation and then less photon impinging on the detector. In principle, by using a powerful source working @ 90 keV, the measurement in 35 cm of water, should give approximately the same results than the measurement in 15 cm of water, independently of the size of the bone. In a large amount of water, large bones will give a stronger signal than small bones.

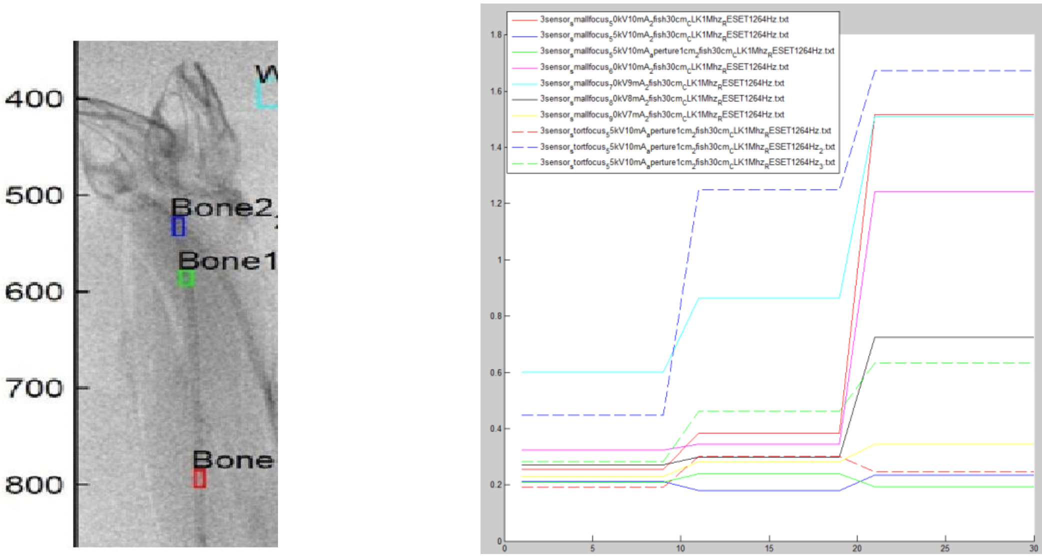

Figure 32: a) Region where signal strength was evaluated; b) Experimental measurement of contrasts obtained in 15 cm of water. (SNR_water - SNR_sample)/(SNR_sample).

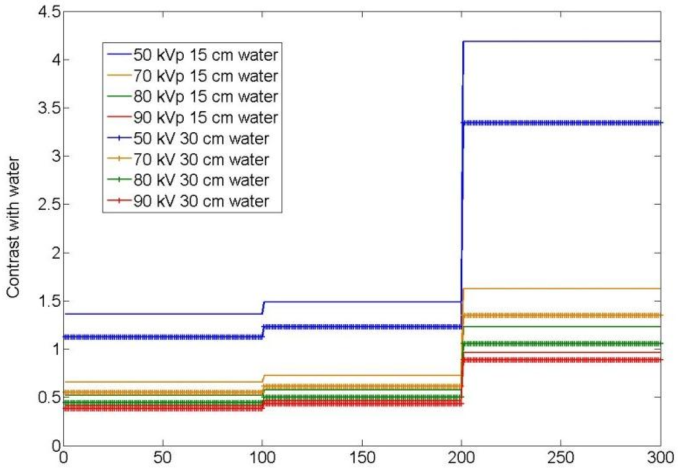

Figure 33: Simulation of x-ray contrast for a 30 cm long fishes in 15 cm and 30 cm of water

2.3.6 Water variation and air bubbles

The variation of the water level in the tube with time, as well as air bubbles will degrades the quality of the images. Strategies for compensating for those artefacts could be the following:

- Use a priori information about the bubble shapes and volume variation. For example, detected small spherical features in the images, that corresponds very probably to air bubbles, and compensate for them by “adding” an amount of calculated x-ray attenuation corresponding to the missing amount of water.
- Volume variation over time or perpendicularly to the longitudinal axes could be compensated for by using the a priori knowledge about the attenuation of x-ray into a full water pipe. Water waves have been smoothed by using dedicated filtering in our trials (see 3.4 for a more detailed description).
- Volume variation could also be measured in real time using ultra sound sensors, laser line scanner or a camera. Knowing the 3D shape of the water surface, one could also compensate for it in the x-ray image by adding the right amount of x-ray attenuation in water

An example of how the water waves affect the image and how it is corrected by image analysis is shown on Figure 34. In the top of the figure, from line 0 to 800, the water is still and the x-ray image is rather uniform apart from different response from the line detectors. As the fish fall in water at line 800 to line 1700, waves and bubble (white regions in the image) are created. On the corrected image, shown on the right, the dorsal bone can be distinguished, in addition to air bubbles that appeared around the line 60.

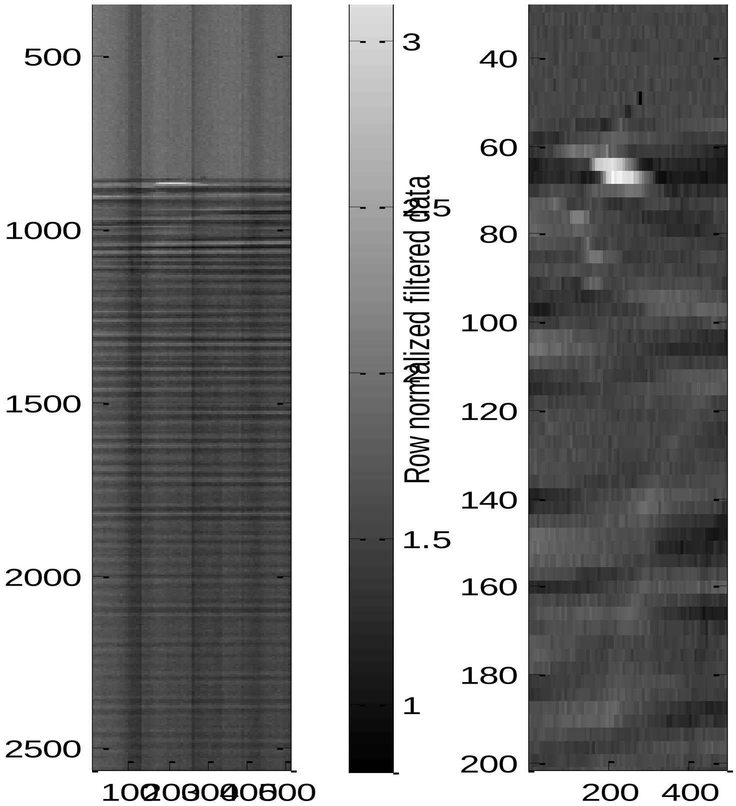

Figure 34: Effect on waves on x-ray image. Left original recording, right corrected for variations in the z- (verical)direction.

2.4 Image analysis

At this stage in the project the image analysis has mainly been to process the images to enhance the contrast between bones and tissue/water to qualitatively judge the possibilities using x-ray for counting fish.
The raw data needs normalizing to remove the effect of unequal sensor elements and uneven x-ray beam intensity. This is done by:

$$normalizedData = \frac{rawData - blackReference}{whiteReference - blackRefernce}$$

In these x-ray images a strong effect on the image intensity is the distance of water plus fish the x-rays have to penetrate. In the experiments there are waves in the water due to the movement, of the bucket containing fish and water, to build up a 2D image. To remove this effect the image is row-wise normalized. This is done by subtracting each pixel in a row by the row's mean

$$rawNormalizedData = normalizedData - rowMean$$

Different filtering approaches have been tested to enhance the signature of the fish's back bone in the images (see Figure 35 for example)

- directional high pass and low pass filtering
- averaging along the time axis to increase signal to noise ratio
- anisotropic filtering extensively used in medical X-ray imaging (for example of this method see Figure 36)

- enhancing structures by using morphological operators

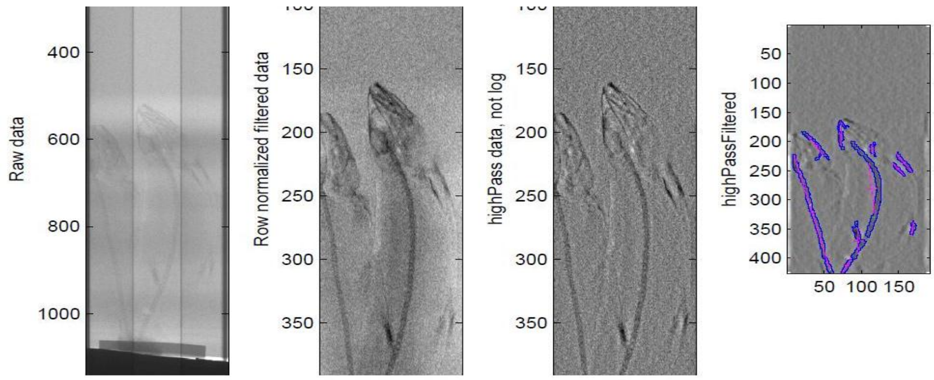

Figure 35: From left: rad data form sensor, black and white reference normalized and row-wise normalising of the data, high pass filtered data, and filtered high pass data with threshold segmented bones.

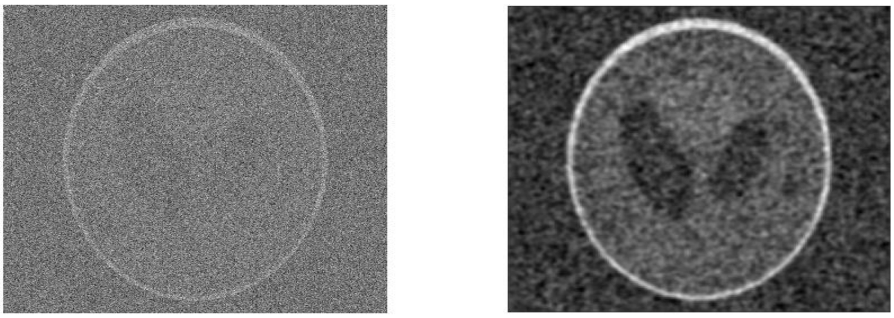

Figure 36: From left: rad data form sensor, black and white reference normalized and row-wise normalising of the data, high pass filtered data, and filtered high pass data with threshold segmented bones.

For segmenting bones in the image the filtered images has been thresholded followed by grouping connected regions into bone regions. The filtered high pass filtered images proved to be the best starting point for this process. Classifying the bone regions into backbones and not backbones has not been performed. As seen in the rightmost image in Figure 35 the backbones are long lines with no or a slight curvature. We expect to fit a second order polynomial to these structures for classification and for grouping back bone segments that has been divided into several smaller segments.

2.5 Summary of the lab-based trials

The lab based experiment have shown that it is possible to detect small to large fishes (800-5 000 grams) in small to large amount of water (15 cm to 35 cm tube diameter) at a speed of at least 1 meters per second with a rather compact set up (of the size of airport x-ray system). Those tests have been performed by a system built using off-the-shelf components.

We have evaluated the following parameters:

-spatial resolution: Both the geometry of the system, the source size and the pixel size should allow a transversal resolution (perpendicular to the tube) of approximately 1 mm.

-Integration time: With a fish speed of 2 m/s, 1 ms allows a longitudinal resolution of 2 mm, which is enough to detect fishes which are several cm long. For small fishes in 15 cm of water, 1 ms gives also an acceptable signal to noise ratio.
-Contrast between fish bone and fishes: This value is approximately equivalent to the contrast between bone and water as water and muscle have approximately the same density and x-ray attenuation properties. With our simulation model a value of 0.15 for 4 cm thick fishes and 0.35 for 10 cm thick fishes were calculated for waterfilled tubes with diameter of 20 cm and 30 cm respectively (contrast calculated as $(SNR_{water} - SNR_{fish})/SNR_{water}$). Values ranging between 0.2 and 1.6 have been measured on smaller fishes in small amount of water.
-X-ray effect and voltage: Voltages between 90 and 160 kV and filament current of at least 5 mA (around 500 W) had to be used to obtain a reasonable signal to noise ratio. This high power is mainly due to the attenuation in a high volume of water and the speed at which the fish have to be detected. However, given the gain that could be achieved using time averaging, and better detector, it should be possible to decrease the power by a factor of two. The voltage however has to be high enough, at least 90 kV, to allow enough x-ray photon to cross the water volume in a short time slot.
-Imaging features of interests for the detection of fishes
The bones of the fishes are obviously the features of choice for the detection of one or several overlapping fishes. The other parameter that could have a real impact is the swim bladder, which gave a very strong contribution to the contrast. The refraction effect at the edge of the fishes could also help in identifying and defining further the position of fishes, especially when imaging with small amount of water.
-Interfering parameters – the effect of air bubbles: This effect is important and has not been fully evaluated since it is has been difficult to document it precisely enough and since it was difficult to simulate with our set up. The only way to assess it correctly would be though tests on a (pseudo) real system. However both simulation and experimental trials show that it can be compensated for to a certain extent. The effect of a simulated of a volume of air between 0 and 10 % randomly distributed in the total volume of water still allows distinguishing a fish from the water.

The work performed in this phase has also resulted in the design and fabrication of a set up that could be transported or reproduced for transportation in the field. Shielding cabinet could be borrowed or bought and adapted to the case of fish counting. Figure 37 shows a picture of the armature, without x-ray source and detectors, which has been used in the experiment before cladding with steel and lead panels. The costs to build infrastructure have been shared by the EXACTUS project and four other x-ray projects. Sensors, sources and other equipment specific for EXACTUS, should be covered by the project alone.

Figure 37: Skeleton of the armature that has been designed for the project and which costs have been partly covered by exactus

2.6 Further improvement for a field utilisation

In our series of experiment we have use detectors that do not follow the geometry of the pipe. In a real system, the detectors will have to follow the curve of the pipe. The geometrical configuration used in all our experiment corresponds to the worst measurement situation, i.e the x-ray beam crosses the pipe along its largest dimension and only the detectors at the centre see the fishes. The lowest SNR case has thus been experimentally simulated, and it is expected that the performances will improved when going from the centre to the periphery. At this last point, the x-ray beam crosses a small amount of water and the SNR is expected to be high. For a given x-ray source power, the effort in increasing the SNR should then be focused on the centre of the pipe. This could be done for example, by using several detectors placed very close together and by summing the signal registered by all. This will add some complexity to the data acquisition, but increase the SNR by a factor equal to the square root of the number of detector, i.e 4 detectors will increase the SNR by a factor of 2. The detected contrast between bone and water is also a parameter that can be further optimized. As shown on paragraph 1.4 the contrast is dependant of the scintillator thickness. It is also dependant of the scintillator type. Optimizing those two parameters will allow increasing the contrast and thus increase the performances of the system. The spectral distribution of the source and its power are also parameters of importance that contributes significantly to the contrast. By letting the distribution of the incoming flux have more weight towards the low energy range, the performances will improve by the increase of the flux of photon that bears more contrast information and by decreasing the flux of photon that contribute most to the noise. Another possibility for improvement lies in the use of a 2D detector with a small number of lines. Increasing both the SNR and the contrast can be obtained by having the successive photodiode lines equipped with different scintillator thickness. Those could be chosen such as to optimize the contrast to noise ratio for the specific task of imaging fish bones in water.

3 References:

Kalivas, Modeling quantum noise of phorphors used in medical X-ray imaging detectors, Nuclear Instruments and methods in Physics Research A 430 (1999)

P. Perona and J. Malik, Scale-Space and Edge Detection Using Anisotropic Diffusion.
IEEE Transactions on Pattern Analysis and Machine Intelligence,
12(7):629-639, July 1990.

G. Grieg, O. Kubler, R. Kikinis, and F. A. Jolesz., Nonlinear Anisotropic Filtering of MRI Data.
IEEE Transactions on Medical Imaging, 11(2):221-232, June 1992.
MATLAB implementation based on Peter Kovesi's anisodiff(.):

P. D. Kovesi. MATLAB and Octave Functions for Computer Vision and Image ocessing.
School of Computer Science & Software Engineering,
The University of Western Australia. Available from:
<http://www.csse.uwa.edu.au/~pk/research/matlabfns/>.

Credits:
Daniel Simoes Lopes
ICIST
Instituto Superior Tecnico - Universidade Tecnica de Lisboa
danlopes (at) civil ist utl pt
http://www.civil.ist.utl.pt/~danlopes
May 2007 original version

Technology for a better society

www.sintef.no